Bioorganic & Medicinal Chemistry Letters xxx (2015) xxx–xxx

Contents lists available at ScienceDirect

Bioorganic & Medicinal Chemistry Letters

journal homepage: www.elsevier.com/locate/bmcl

Diversification of edaravone via palladium-catalyzed hydrazine cross-coupling: Applications against protein misfolding and oligomerization of beta-amyloid

Mark A. MacLean [a], Elena Diez-Cecilia [b], Christopher B. Lavery [a], Mark A. Reed [c], Yanfei Wang [b], Donald F. Weaver [a,b,c,*], Mark Stradiotto [a,*]

[a] Department of Chemistry, Dalhousie University, 6274 Coburg Road, PO Box 15000, Halifax, NS B3H 4R2, Canada
[b] Toronto Western Research Institute, University Health Network, University of Toronto, Krembil Discovery Tower, 4th Floor 4KD-472, 60 Leonard Avenue, Toronto, ON M5T 2S8, Canada
[c] Treventis Corporation, 1411 Oxford Street, Halifax, NS B3H 3Z1, Canada

ARTICLE INFO

Article history:
Received 7 September 2015
Revised 5 November 2015
Accepted 8 November 2015
Available online xxxx

Keywords:
Alzheimer's disease
Beta-amyloid
Palladium-catalyzed aminations
Hydrazine

ABSTRACT

N-Aryl derivatives of edaravone were identified as potentially effective small molecule inhibitors of tau and beta-amyloid aggregation in the context of developing disease-modifying therapeutics for Alzheimer's disease (AD). Palladium-catalyzed hydrazine monoarylation protocols were then employed as an expedient means of preparing a focused library of 21 edaravone derivatives featuring varied *N*-aryl substitution, thereby enabling structure–activity relationship (SAR) studies. On the basis of data obtained from two functional biochemical assays examining the effect of edaravone derivatives on both fibril and oligomer formation, it was determined that derivatives featuring an *N*-biaryl motif were four-fold more potent than edaravone.

Alzheimer's disease (AD) is a progressive neurodegenerative disorder, leading to cognitive impairment, memory loss and ultimately dementia.[1] Currently, more than 25 million people worldwide are afflicted with AD, a number that will quadruple by 2050.[2,3] While current treatments offer temporary, symptomatic improvement, 'curative' therapies that can arrest the progression of AD are currently unavailable. The aberrant misfolding and aggregation of beta-amyloid (Aβ), arising from cleavage of amyloid precursor protein, is central to the pathogenesis of AD.[1,2,4] Accordingly, the development of drug-like small molecules that can penetrate the blood–brain barrier and interfere with Aβ aggregation, thereby inhibiting the assembly of neurotoxic oligomers, represents a promising disease-modifying therapeutic approach.

As part of our on-going research program to evaluate known drug-like molecular platforms as putative therapeutics against protein misfolding, we identified multiple chemotypes that included *N*-aryl pyrazolones such as edaravone (**1**, Scheme 1). The neuroprotective characteristics of edaravone are well-described; the potent anti-oxidant and free-radical scavenging properties of this compound have been exploited therapeutically to reduce neuronal damage associated with acute brain ischemia.[5] Moreover, since oxidative stress is known to figure prominently in the pathogenesis of AD,[6] we became interested in preparing and assessing the anti-aggregation properties of edaravone and related analogs.

In preliminary work, *N*-aryl substituents emerged as a key pharmacophore, and therefore an important locale for diversification and structure–activity relationship (SAR) studies. Whereas structural modification at the R position can be achieved by use of established methods and commercial reagents (Scheme 1), variation at the sp^2-hybridized *N*-aryl position requires access to structurally diverse monoaryl hydrazine synthons of the aryl-$NHNH_2$ type. Conventional protocols employed for the formation of monoaryl hydrazines include nucleophilic aromatic substitution involving an activated aryl halide,[7] as well as diazotization of aniline derivatives followed by reduction of the resulting diazonium salt.[8] While feasible,[9] such protocols can be viewed as being problematic in terms of limited substrate scope, harsh reaction conditions, and poor atom economy.

Abbreviations: AD, Alzheimer's disease; Aβ, amyloid beta; ThT, Thioflavin T; bio-$Aβ_{42}$, *N*-α-biotinyl-Aβ (1–42); SAR, structure activity relationship; OFB, oligomer formation buffer.

* Corresponding authors. Tel.:+1 416 603 5867, +1 902 494 7190.
E-mail addresses: weaver@uhnres.utoronto.ca (D.F. Weaver), mark.stradiotto@dal.ca (M. Stradiotto).

http://dx.doi.org/10.1016/j.bmcl.2015.11.022
0960-894X/

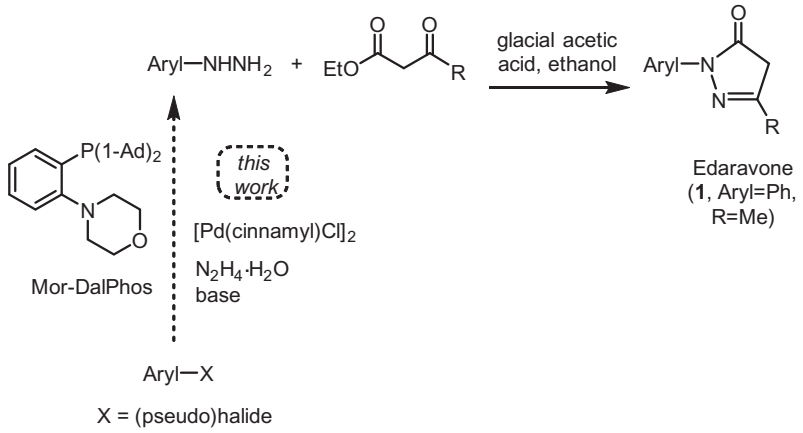

Scheme 1. Synthetic route to edaravone and related *N*-aryl derivatives.

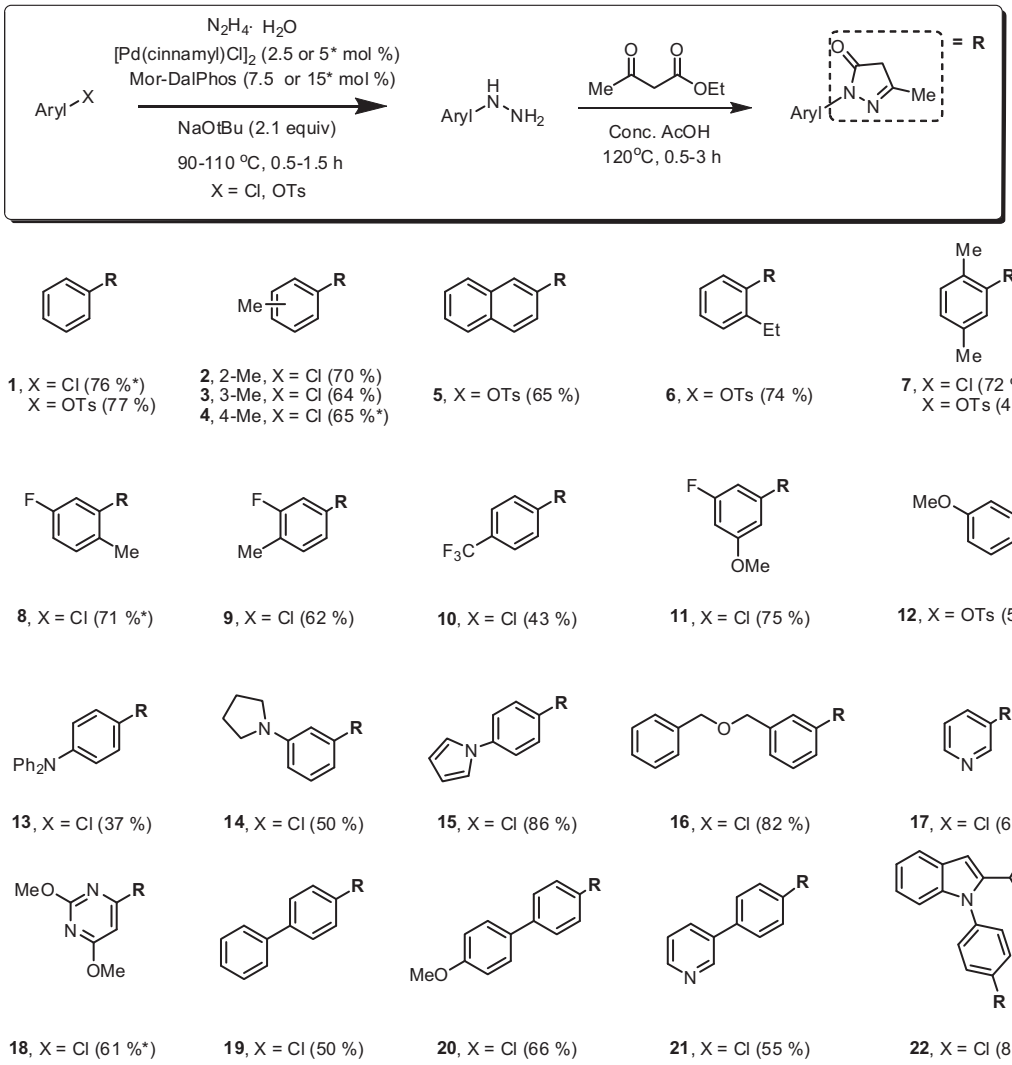

Figure 1. Preparation of edaravone derivatives employing palladium-catalyzed hydrazine cross-coupling methodology.

Given the broad utility of monoaryl hydrazines in the assembly of myriad heterocyclic scaffolds,[10] the identification of modular synthetic methods for the preparation of such synthons directly from (hetero)aryl (pseudo)halides and convenient hydrazine sources (e.g., $N_2H_4{\cdot}H_2O$) represents an important synthetic challenge that until very recently remained unaddressed.[11] Whereas Buchwald–Hartwig amination methods would appear to be well-suited for (hetero)aryl hydrazine synthesis, the strongly reducing nature of hydrazine presents a formidable challenge, both with respect to unwanted hydrodehalogenation of the (hetero)aryl (pseudo)halide

Table 1
Amyloid beta anti-aggregation screening data for **1–22**

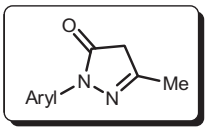

Compd	Aryl	% inh $A\beta_{40}$ at 25 μM[a]	$A\beta_{40}$ IC_{50}[a] (μM)	Bio-$A\beta_{42}$ IC_{50}[a] (μM)	Compd	Aryl	% inh $A\beta_{40}$ at 25 μM[a]	$A\beta_{40}$ IC_{50}[a] (μM)	Bio-$A\beta_{42}$ IC_{50} (μM)[a]
1		17.2	ND[b]	>50	**12**	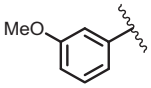	39.7	>50	>50
2		22.7	ND[b]	>50	**13**	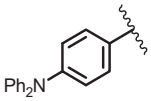	50.7	>50	4.0
3	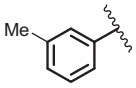	30.9	ND[b]	>50	**14**	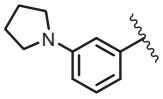	47	ND[b]	16.8
4	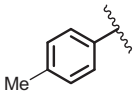	16.3	ND[b]	>50	**15**	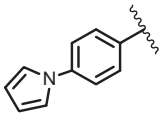	60.6	26.0	4.0
5	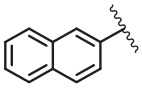	56.2	ND[b]	>50	**16**	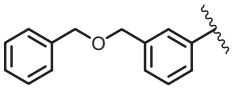	53.4	27.0	2.9
6		26.3	ND[b]	>50	**17**		20.2	ND[b]	>50
7	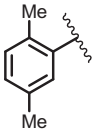	7.4	ND[b]	>50	**18**	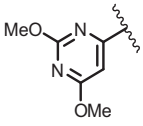	48.2	ND[b]	>50
8	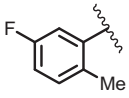	26.2	ND[b]	>50	**19**	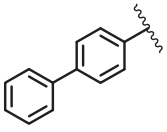	78.7	5.6	19.5
9	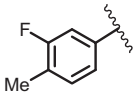	49.0	ND[b]	>50	**20**	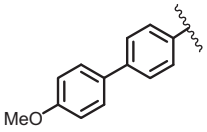	69.6	3.4	5.1
10	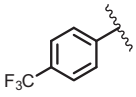	56.3	ND[b]	>50	**21**	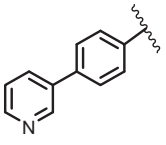	53.2	14.5	3.9
11	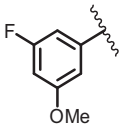	26.4	ND[b]	>50	**22**	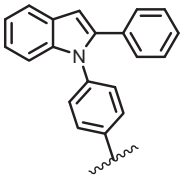	71.4	19.6	3.5

[a] Full details of the experimental protocols employed in these assays and SEM are provided in the accompanying Supplementary data.
[b] ND = not determined. IC_{50} values were only collected for the most active compounds with >50% inhibition at 25 μM in the $A\beta_{40}$-ThT assay and an IC_{50} value of <50 μM in the bio-$A\beta_{42}$.

reagent, as well as formation of catalytically inactive palladium black. Despite such challenges, the first reported protocol of this type was disclosed by one of our research groups in 2010.[12] Key to the success of this transformation was the use of [Pd(cinnamyl)Cl]$_2$/Mor-DalPhos catalyst mixtures, which were employed in the cross-coupling of inexpensive and readily obtained (hetero)aryl chlorides and tosylates, thereby affording structurally diverse monoaryl hydrazine derivatives in synthetically useful yields.

Herein we report on the application of this novel cross-coupling strategy toward the modular assembly of a small library of edaravone derivatives featuring variation in the *N*-aryl substituent, and the subsequent assessment of the abilities of such *N*-aryl pyrazolones to inhibit $A\beta_{40/42}$ aggregation. The protocol employed in preparing a small library of edaravone derivatives is depicted in Figure 1.

This procedure makes use of the palladium-catalyzed cross-coupling of (hetero)aryl chlorides or tosylates with hydrazine hydrate to afford the requisite monoaryl hydrazine intermediate, followed by treatment with ethyl acetoacetate under acidic conditions to afford the desired pyrazolone. In exploiting this modular strategy, the expedient synthesis of edaravone derivatives featuring a diversity of substitution patterns at the *N*-aryl position was achieved (Fig. 1). Edaravone itself (**1**) was prepared in this manner in good yield (76% from PhCl; 77% from PhOTs), as were isomeric *N*-tolyl (**2**–**4**) and naphthyl (**5**) compounds. *Ortho*-ethyl substitution was well accommodated (**6**), as was 2,5-dimethyl substitution (**7**, albeit in lower yield when employing the aryl tosylate). Edaravone derivatives featuring *N*-phenyl groups comprising a combination of methyl, fluoro, trifluoro and/or methoxy substituents (**8**–**12**) were each prepared in acceptable isolated yield, as were derivatives featuring amine and ether addenda (**13**–**16**). While heteroaryl (pseudo)halides in general proved to be challenging reaction partners in this cross-coupling chemistry (including heteroaryl chlorides derived from thiophene, imidazole, or quinoline), pyrazolones featuring pyridine or pyrimidine groups at nitrogen were prepared successfully in good isolated yield (**17**–**18**). Finally, given the privileged nature of the biaryl motif in pharmaceutical chemistry,[13,14] we directed our attention to the preparation of such edaravone derivatives. *N*-(hetero) biaryl pyrazolones featuring methoxy, pyridyl, and indolyl functionalities were all synthesized successfully (**19**–**22**). Notably, 15 of the edaravone derivatives prepared herein represent new compounds that had not been reported previously in the chemical literature, thereby underscoring the utility of the expedient palladium-catalyzed methodology employed.

With a small focused library of edaravone analogs in hand, we next investigated their ability to inhibit aggregation of Aβ in vitro. For this purpose, we selected two functional biochemical assays to study the effect of each compound on both fibril and oligomer formation. To monitor fibril or larger aggregate formations that are rich in beta-sheet conformation, analogs were screened using the fluorescent dye-binding agent Thioflavin T (ThT).[15] Briefly, $A\beta_{40/42}$, in its monomeric form, is soluble in solution at physiological temperature and pH, and takes a predominantly α helical/random coil structure. Following the process of misfolding and self-association, mature aggregates/fibrils can be formed that are enriched in cross-β pleated sheets. ThT, a benzothiazole dye, has a strong affinity for proteins with high β-sheet content, and as such may be used to visualize Aβ aggregates. Unbound ThT has fluorescence excitation (λ_{ex}) and emission (λ_{em}) wavelengths of 430 and 342 nm, respectively; upon binding to amyloid fibrils, ThT undergoes a characteristic spectral shift (λ_{ex} 442 nm, λ_{ex} 482 nm), which can be used to differentiate bound and unbound ThT. Using a kinetic aggregation assay format,[16] compounds were incubated at a single concentration of 25 μM with $A\beta_{40}$ (20 μM) in the presence of ThT (8 μM) and fluorescence measurements were taken over a period of 72 h. $A\beta_{40}$ was chosen over $A\beta_{42}$ due its ease of handling and the reproducibility of this particular assay system. The percentage inhibition of $A\beta_{40}$ aggregation (measured at 72 h) by the analog series, is shown in Table 1.

We next screened the compounds through a biochemical assay specifically designed to monitor the formation of smaller, neurotoxic-associated oligomers. This was achieved using an assay system developed by Levine[17] that measures sub-nanomolar concentrations of $A\beta_{42}$ oligomers utilizing biotin-labeled $A\beta_{42}$ protein. This robust assay system specifically recognizes multimeric (>20 kDa) oligomers of *N*-α-biotinyl-Aβ(1–42) (bio-$A\beta_{42}$) but not monomeric bio-$A\beta_{42}$ via a single-site NeutrAvidin capture/labeled streptavidin detection configuration. Compounds **1**–**22** were screened in this assay system using a concentration range of 1–50 μM to generate a dose response curve from which IC_{50} values were determined.

Analyzing the data in Table 1, compounds **1**–**12**, **17** and **18**, which lack aromatic functionality outside of the phenyl pyrazolone core, show no effect on inhibiting oligomerization in the bio-$A\beta_{42}$ assay (IC_{50} > 50 μM). The same compounds show weak to moderate activity in the $A\beta_{40}$-ThT assay system, with compounds **5**, **9**, **10** and **18** exhibiting in the range of 50% inhibition at 25 μM. The only outlier in this context is the pyrrolidine **14**, which shows 47% inhibition at 25 μM ($A\beta_{40}$-ThT) and IC_{50} = 16.8 μM (bio-$A\beta_{42}$). Most interestingly, increased potency is observed in both assays when aromaticity is introduced in the *para* position of the *N*-aryl pyrazolone. Compounds **19**–**21** all display strong inhibition with IC_{50} values in both assay system in the low micromolar range (see Table 1). The $A\beta_{40}$-ThT and bio-$A\beta_{42}$ dose response curves for **20** are shown in Figure 2.

Similar activity profile was also observed with the *N*-linked aromatic heterocycles **15** ($A\beta_{40}$-ThT, IC_{50} = 26.0 μM; bio-$A\beta_{42}$, IC_{50} = 4.0 μM) and **22** ($A\beta_{40}$-ThT, IC_{50} = 19.6 μM; bio-$A\beta_{42}$, IC_{50} = 3.53 μM). Interestingly, the diphenyl aniline **13** demonstrated similar anti-oligomer activity (bio-$A\beta_{42}$, IC_{50} = 4.0 μM), but considerably lower inhibition in the ThT aggregation system ($A\beta_{40}$-ThT, IC_{50} > 50 μM), indicating a potential separation in oligomer versus larger aggregate inhibitory effects. Adding further evidence that additional aromaticity needs to be positioned further out from the phenyl pyrazalone structure, the benzyl ether **16**

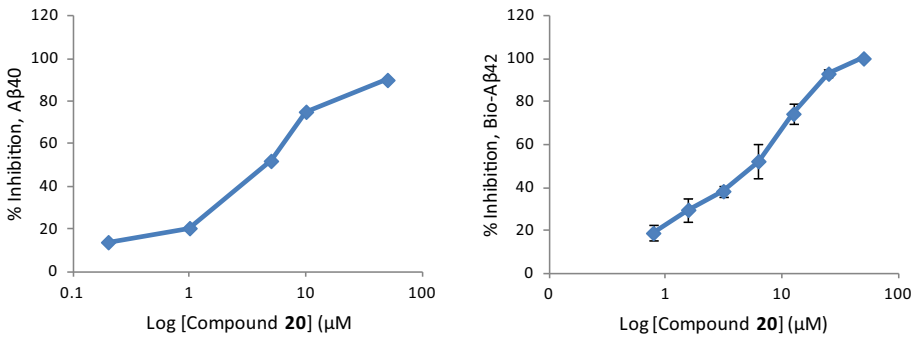

Figure 2. Dose–response curves of the percentage of inhibition of $A\beta_{40}$ and bio-$A\beta_{42}$ of compound **20**.

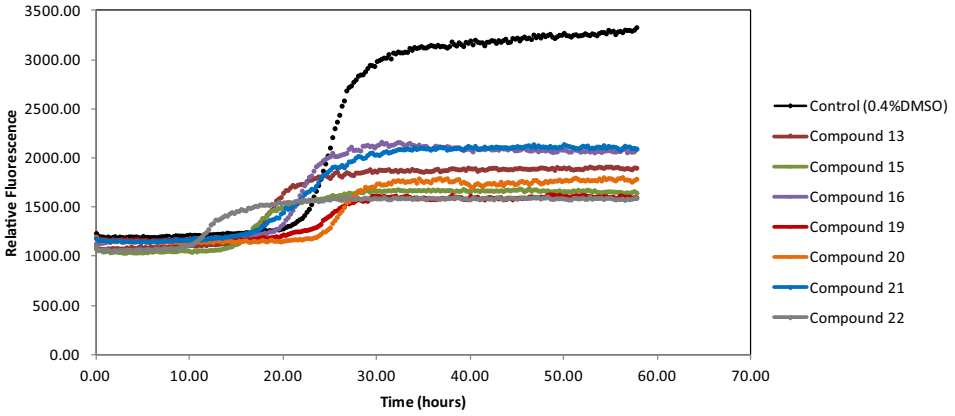

Figure 3. Thioflavin T kinetic curves for the most active compounds against $A\beta_{40}$ **13**, **15**, **16**, **19**–**22** at 25 μM concentration.

showed potent $A\beta_{42}$ oligomer inhibition (bio-$A\beta_{42}$, IC_{50} = 2.9 μM) and moderate activity in ThT assay (IC_{50} = 27 μM). The single concentration ThT inhibition for the most active compounds in this series is shown in Figure 3.

Considering the biological data obtained, various SAR conclusions can be put forth. Functionalization of the phenyl ring attached to the pyrazolone with alkyl, methoxy or fluorinated substituents, or the exchange of one or more hydrogens of the phenyl ring for nitrogen, does not enhance the anti-aggregant activity of the compounds versus edaravone (**1**) itself. Conversely, introducing aromaticity in the *N*-aryl pyrazolone at any of the positions studied increased compound potency exponentially as both $A\beta_{40}$ and bio-$A\beta_{42}$ antiaggregants. Equivalently, high misfolding activity was found with compounds possessing an *N*-linked heterocycle attached to the *N*-aryl pyrazolone.

Although our lead compounds successfully inhibit the oligomerization and aggregation of both $A\beta_{40}$ and bio-$A\beta_{42}$ with IC_{50} values in the low micromolar range, due to poor preliminary in vitro pharmacokinetic and pharmacodynamics properties (very low microsomal stability and poor cell penetration), this class of compounds was not subjected to any further lead optimization.

In conclusion, we have demonstrated the utility of employing palladium-catalyzed cross-coupling methodologies in the expedient synthesis of monoaryl hydrazines for use in the assembly of edaravone derivatives with application in inhibiting the aberrant folding and aggregation of Aβ. The *N*-aryl pyrazolone motif offers immense therapeutic value due to their broad biological spectrum which includes antimicrobial, antibacterial, antiinflammatory, antitumor, antidepressant and neuroprotective activity.[18] For these reasons, efficient synthetic routes to novel pyrazolones, as described in this work, offer significant advantages in the design and generation of small bioactive molecule libraries.

Acknowledgements

The authors are grateful to the Canadian Institutes of Health Research (CIHR) and Natural Science and Engineering Research Council (NSERC) for financial support.

Supplementary data

Supplementary data associated with this article can be found, in the online version, at http://dx.doi.org/10.1016/j.bmcl.2015.11.022.

References and notes

1. Goedert, M.; Spillantini, M. G. *Science* **2006**, *314*, 777.
2. Hamley, I. W. *Chem. Rev.* **2012**, *112*, 5147.
3. Kepp, K. P. *Chem. Rev.* **2012**, *112*, 5193.
4. Hardy, J.; Selkoe, D. J. *Science* **2002**, *297*, 353.
5. Yoshida, H.; Yanai, H.; Namiki, Y.; Fukatsu-Sasaki, K.; Furutani, N.; Tada, N. *CNS Drug Rev.* **2006**, *12*, 9.
6. Yan, Y. F.; Gong, K.; Ma, T.; Zhang, L. H.; Zhao, N. M.; Zhang, X. F.; Tang, P. F.; Gong, Y. D. *Neurosci. Lett.* **2012**, *531*, 160.
7. Allen, C. F. H. *Org. Synth.* **1933**, *13*, 36.
8. Coleman, G. H. *Org. Synth.* **1922**, *2*, 71.
9. Nakagawa, H.; Ohyama, R.; Kimata, A.; Suzuki, T.; Miyata, N. *Bioorg. Med. Chem. Lett.* **2006**, *16*, 5939.
10. Robinson, B. *Chem. Rev.* **1963**, *63*, 373.
11. Stradiotto, M. In *New Trends in Cross-Coupling: Theory and Application*; Colacot, T. J., Ed.; Royal Society of Chemistry: Cambridge, UK, 2014; pp 228–253.
12. Lundgren, R. J.; Stradiotto, M. *Angew. Chem., Int. Ed.* **2010**, *49*, 8686.
13. Horton, D. A.; Bourne, G. T.; Smythe, M. L. *Chem. Rev.* **2003**, *103*, 893.
14. Hajduk, P. J.; Bures, M.; Praestgaard, J.; Fesik, S. W. *J. Med. Chem.* **2000**, *43*, 3443.
15. Levine, H., III *Methods Enzymol.* **1999**, *309*, 274.
16. (a) Chalifou, R. J.; McLaughlin, R. W.; Lavoie, L.; Morissette, C.; Tremblay, N.; Boulé, M.; Sarazin, P.; Stéa, D.; Lacombe, D.; Tremblay, P.; Gervais, F. *J. Biol. Chem.* **2003**, *278*, 3487; (b) Meek, A. R.; Simms, G. A.; Weaver, D. F. *Can. J. Chem.* **2012**, *90*, 1.
17. (a) Levine, H., III *Anal. Biochem.* **2006**, *356*, 265; (b) Levine, H., III; Ding, Q.; Walker, J. A.; Voss, R. S.; Augelli-Szafran, C. E. *Neurosci. Lett.* **2009**, *465*, 99.
18. Gupta, P.; Gupta, J. K.; Halve, A. K. *IJPSR* **2015**, *6*, 2291.